Dynamic tensile testing of ligaments from the human cervical spine

V.P.W. Shim*, J.F. Liu* and V.S. Lee[+]

*Impact Mechanics Laboratory
Department of Mechanical Engineering
National University of Singapore
10 Kent Ridge Crescent, Singapore 119260, Republic of Singapore

[+]Defence Medical and Environmental Research Institute
DSO National Laboratories
27 Medical Drive, Singapore 117510, Republic of Singapore

ABSTRACT This study focuses on establishing appropriate experimental methodology to facilitate investigation of the dynamic stress-strain characteristics of soft bio-tissues. Dynamic mechanical tests were conducted on ligaments from the human cervical spine (neck), using a tensile split Hopkinson bar device. The strain rates imposed were of the order of 10^2~10^3/s. As ligaments are extremely soft and extensible, specific test protocols relating to Hopkinson bar testing were developed to enable the acquisition of reliable and accurate data. These encompass aspects such as detection of transmitted waves of small magnitudes, a means to perform tests with absolutely zero preloading, and generation of a sufficiently long loading pulse. Comparison with static test results reveals that the initial physiologic (toe) region for dynamic loading is noticeably shorter, while the accompanying stress levels and strength are elevated and able to attain values more than two to three times the static values. However, the elongation capacity of ligaments under dynamic loading is reduced. Simple empirical equations were found to provide suitable fits to the response prior to attainment of the ultimate stress.

Keywords: Cervical spine, ligament, strain rate, Hopkinson bar.

Introduction

There is an increasing number of studies on the quasi-static mechanical properties of ligaments from animal and human sources. The realization that such soft-tissues exhibit rate-sensitive behavior, coupled with concerns over injuries arising from common activities that involve rapid motion, has motivated attempts to investigate their dynamic responses. Quasi-dynamic tests have been performed using universal hydraulic testing machines [1-4], which are able to impose strain rates of up to about 10/s. However, in situations of high speed trauma such as impacts and collisions, ligaments are subjected to much higher rates of stretching. Crowninshield [5] estimated that the medial collateral ligament in a knee may encounter strain-rates of up to 1500/s in automobile impacts at 10m/s; he performed tests at extension rates of up to 5.1m/s (corresponding to a strain rate of 510/s) using a drop hammer loading device.

The human cervical spine is the upper portion of the spine, and is vulnerable when subjected to trauma that arises in situations such as vehicular accidents, sports or pilot ejection. Quasi-static testing of the whole cervical column or partial segments to determine the tensile, compressive, torsional or flexural responses have been undertaken previously [6-8]. Experimental studies on dynamic response under impact loading such as whiplash, relate to injuries induced on the entire spinal column [9-11]. With regard to the mechanical properties of spinal ligaments, some papers have described their tensile properties under quasi-static stretching [12-14]. Yoganandan [15] tested the *ligamentum flavum* and anterior longitudinal ligaments in the human cervical spine at extension rates up to 2.5m/s using a test device that had an electrohydraulic piston; Panjabi [16] tested the *alar* and transverse ligaments at speeds of 0.9m/s by means of equipment involving a gas-driven piston. Significant rate-dependence of the mechanical behavior was found. The present study employs a tensile split Hopkinson bar arrangement to measure the dynamic properties of ligaments. The split Hopkinson bar is a commonly-used device to obtain the dynamic stress-strain characteristics of material at approximately constant strain rates. It is usually used for tests on materials which have an acoustic or mechanical impedance that is comparable with the input/output bars. However, ligaments are extremely soft and flexible and possess a very low mechanical/wave impedance. Consequently, tests on such materials would pose severe difficulties. There is a dearth of information on dynamic testing of compliant biological materials such as ligaments, especially with regard to the use of Hopkinson bar devices. Therefore, the present effort focuses on the development of special techniques to make Hopkinson bar systems suitable for accurate and reliable testing of such materials. These encompass aspects such as specimen preparation, detection of transmitted waves of small magnitudes, a means to perform tests with absolutely zero preloading, and generation of a sufficiently long loading pulse. Typical results show stress-strain curves of ligaments that commence with a nonlinear toe region leading to an almost linear elastic response before failure.

Compared to static responses, the dynamic stress-strain curves of ligaments exhibit an elevation in strength but reduced elongation.

Ligament specimen preparation

The human cervical spine is an articulate structure comprising seven vertebrae, denoted by C1 to C7 (Fig.1). C2 to C7 are connected to one another by intervertebral discs and ligaments, while C0, C1 and C2 are connected only by ligaments. Detailed anatomic descriptions of the cervical spine and associated ligament structures can be found in [17]. In this study, the cervical spines were stored at a temperature of around -30^{o}C with muscles intact to prevent decay and dehydration of the ligaments. For specimen preparation, each spine was thawed at room temperature and the muscles removed; saline solution was sprayed to keep the tissues moist. The means for clamping the ends of a specimen for tensile testing is a major concern with regards to soft biological samples. Cryogenic methods of fixation have been used by some researchers [18]. However, the resulting temperature gradients generated in soft tissue specimens will alter their mechanical properties. This poses problems if the specimens are short, such as ligamentous samples from the cervical spine. Consequently, bone-ligament-bone units are utilized as tensile specimens in the present study. As the stiffness of bone is much larger than that of ligament, any error caused by deformation of bone ends during loading is negligible. To attach a specimen to the input/output bars of the Hopkinson bar device, clamping adapters of the same diameter and material were designed (Fig. 1). Each bone end was inserted into the cavity of an adapter and dental cement was used to fill the remaining space to fix the bone to the adapter. This also helped minimize mechanical impedance mismatch between the adapters and the bars. For stronger ligaments with larger bone ends, a threaded pin was used to reinforce the adapters. The adapter-specimen unit was then screwed tightly into the input and output bars, and tensile tests then carried out. Specimens were prepared such that the applied tension aligned with the physiological loading direction.

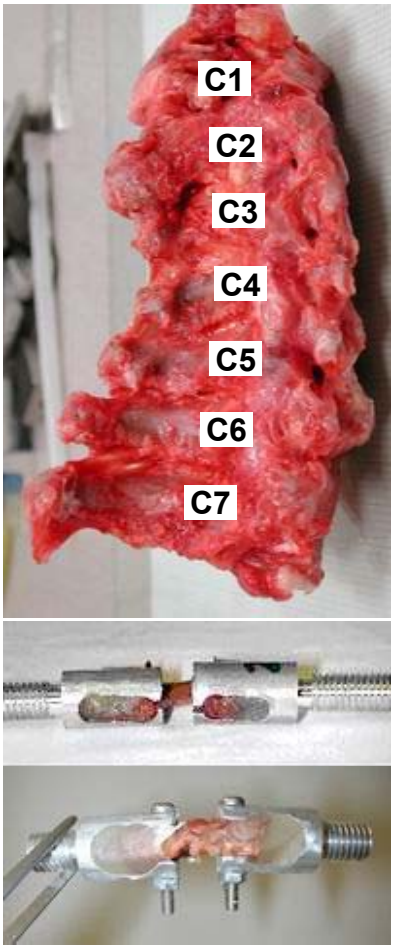

Fig.1 Cervical spine and fixation of bone-ligament-bone unit for Hopkinson bar testing.

Experimental procedure

Split tensile Hopkinson bar system

Lindholm [19] has listed parameters relevant to the classification of mechanical tests according to strain rate. For high strain rates of the order of 10^2~10^3/s, inertial forces are important and wave propagation must be taken into consideration. For such cases, conventional load cells are unable to measure the force history in specimens because the force detected by the load cell may not be that experienced by the specimen. This is because the loading wave is distorted by internal reflection within the complex structure of the load cell. The split Hopkinson bar system was established for performing tests at strain rates of 10^2/s to 10^3/s. This technique, formulated by Kolsky [20], is able to determine dynamic stress-strain relationships for materials at relatively constant strain-rates. Long input/output bars facilitate the generation and propagation of one-dimensional stress waves with relatively little distortion, and small strain gages can be conveniently mounted on them to measure the dynamic strains induced. A schematic diagram of the tensile Hopkinson bar system used in this study is given in Fig. 2. A tubular striker is accelerated by pressurized air, causing it to impact the target cap and generate a force pulse with an approximately rectangular profile in the input bar. This pulse corresponds to an incident strain wave $\varepsilon_i(t)$ that propagates along the input bar until it reaches the bar-specimen interface x_1. Subsequently, part of the incident wave passes through the specimen into the output bar as a transmitted wave $\varepsilon_t(t)$ and part of it is reflected back from the interface as a reflected wave $\varepsilon_r(t)$. The average stress, strain-rate and strain in the specimen are obtained by averaging the stress and velocity histories at both ends of the specimen. Based on the assumption of one-dimensional stress wave propagation, these quantities are determined from the input, transmitted and reflected strain histories recorded by strain gages on the input/output bars:

$$\sigma_s(t) = \frac{A_0}{2A_s}\left[\sigma(x_1,t)+\sigma(x_2,t)\right] = \frac{E_0 A_0}{2A_s}\left[\varepsilon_i(t)+\varepsilon_r(t)+\varepsilon_t(t)\right]$$
$$\dot{\varepsilon}_s(t) = \frac{v(x_1,t)-v(x_2,t)}{L_s} = \frac{C_0}{L_s}\left[\varepsilon_i(t)-\varepsilon_r(t)-\varepsilon_t(t)\right] \qquad (1)$$
$$\varepsilon_s(t) = \int_0^t \dot{\varepsilon}_s(t)dt = \frac{C_0}{L_s}\int_0^t \left[\varepsilon_t(t)-\varepsilon_r(t)-\varepsilon_t(t)\right]dt$$

where L_s and A_s denote respectively the gage length and cross-sectional area of the specimen, and A_0, C_0 and E_0 refer respectively the cross-sectional area, elastic wave velocity and modulus of the bar material.

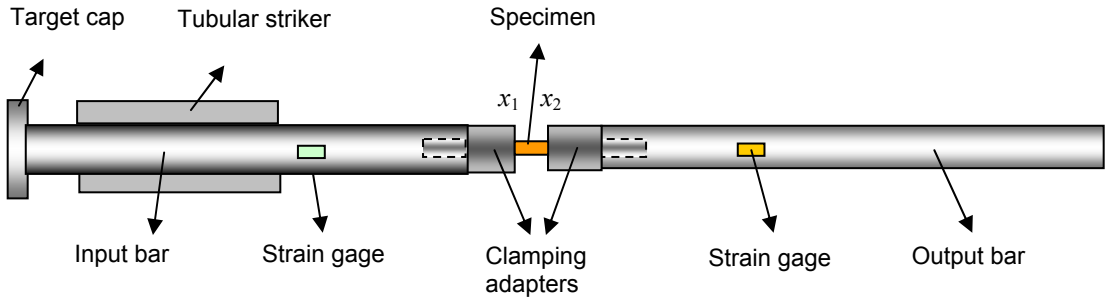

Fig 2. Schematic diagram of a split tensile Hopkinson bar

Modifications for testing of ligaments

The traditional split Hopkinson bar system is generally widely employed in the testing of conventional materials such as metals, plastics, etc, whereby there is a good match between the mechanical impedances of the specimen and the bar material. However, soft biological tissues are extremely pliable and possess a much lower strength compared to most conventional materials. These characteristics pose three main difficulties in Hopkinson bar testing: (1) obtaining reliable readings from the extremely small transmitted wave signals; (2) a proper procedure to ensure an initial zero pre-load on ligament specimens, accompanied by an appropriate method of data processing to capture the entire initial toe response region; (3) generation of a sufficiently long incident wave to stretch compliant specimens to failure, given existing constraints on equipment size.

(1) Use of magnesium bars and semiconductor strain gages

Taking into account the cross-sectional area (*A*) of a structure transmitting a wave, the mechanical or wave impedance is defined by the product of the cross-section, material density and elastic wave velocity (ρCA). For a split Hopkinson bar system, the proportion of the incident wave that is reflected or transmitted is determined by the ratio of the wave impedances between the bar and specimen. A specimen with a low wave impedance causes most of the incident wave to be reflected back; this renders the transmitted wave too small to be detected by common foil strain gages on the output bar. A method that employs a tubular aluminum output bar to decrease the bar cross-sectional area, thus lowering its wave impedance, has been attempted [21]; this requires the attachment of a cap to the end of the tubular output bar for connection to the specimen. To completely reduce wave impedance mismatch between the bar and specimen, it may be possible to utilize polymer input/output bars for testing soft materials. This has the potential of causing the input, reflected and transmitted waves to be of comparable amplitudes. However, extraction of usable data would be quite complex because polymers are viscoelastic and would cause wave dispersion and attenuation [22, 23]. An advantage of metallic bar systems is that the associated equations for data processing are simple, because wave distortion is generally minimal and the stress-strain relationship of the bar material is linear. Consequently, in this study, input/output bars made of a lighter metal – magnesium (1810kg/m^3) – were employed. Static tests show that magnesium has a linear elastic limit of around 120MPa and a Young's modulus of 43.8 GPa. This endows it with a wave impedance only 0.226 times that of steel and 0.65 times that of aluminum. The lower wave impedance and Young's modulus of magnesium contribute to increasing the proportion and amplitude of the wave transmitted to the output bar. However, this is still not sufficient. Figure 3 shows actual strain values induced in magnesium bars (12.5mm

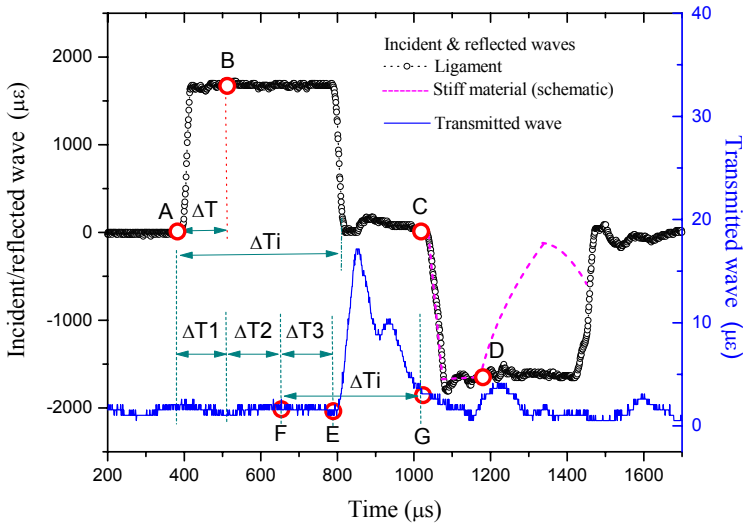

Fig.3 Actual strain magnitudes of incident/reflected and transmitted waves recorded respectively by foil and semiconductor gages, for a tensile test on an anterior longitudinal ligament.

diameter) in a tensile test on an anterior longitudinal ligament (4.2mm gage length). The transmitted wave is only 17 $\mu\varepsilon$ in amplitude, or around 1% of the incident and reflected waves. Accuracy of the stress history experienced by a specimen is governed by the recorded transmitted wave. Hence, accuracy and good resolution in this signal are critical. If conventional foil gages are used, the transmitted signal would be indiscernible from electrical noise. Therefore, another modification implemented is the use of semiconductor strain gages which have very high sensitivity. Semiconductor gages generally have a gage factor of more than 100; this improves the signal-to-noise ratio by more than fifty times that of foil gages with a gage factor of only around 2. In this investigation, a pair of semiconductor gages (gage factor of 130) was mounted diametrically opposite each other on the output bar to record the transmitted wave. The strain in the input bar was still captured using (less costly) foil strain gages, as the input wave was sufficiently large. The signals in Fig. 3 and Fig. 4b (for tests on ALL and ISL specimens) demonstrate that the modifications described enabled accurate capture of the relevant waves.

(2) Testing of specimens with initial slack

A typical load-deformation curve for a soft bio-material (e.g. ligament) comprises an initial exponential-like toe regime, a linear elastic response and final rupture. The stiffness in the initial toe is so low that a very small force induces a large deformation. The static stress-strain curves in Fig.5 and Fig.6 illustrate the toe regime of *alar* and transverse ligaments, and the window in Fig.6 is a magnification of the response near the origin. It is evident that any intentional or inadvertent small preload will shorten the length of this toe regime, introducing inconsistency into the results. The toe regime is associated with the physiological range of movement of a ligament and is an essential component in the complete stress-strain curve. Thus, in this study, a protocol to ensure zero pre-load is implemented both in static and dynamic testing. This is relatively easy to achieve in static testing, as the initial load can be accurately determined. However, when using a split Hopkinson bar, there is no convenient means of identifying the initial force on a specimen after mounting it between the input and output bars. Manual pulling of the bars via a high-sensitivity force sensor does not provide an accurate reading because friction between the bars and its supports cannot be factored out. Consequently, a test method which incorporates initial slack in a specimen was established to achieve a zero pre-load condition and facilitate capture of the entire toe regime.

Traditionally, in tensile Hopkinson bar tests, the specimen is aligned straight and clamped between the input and output bars. In the present study, the ligament specimen is made to have an initial slack between the bars to ensure that there is no load prior to testing. The aspects of concern are the initial degree of slackness, bearing in mind the limited loading duration, and how this affects wave propagation. Initial slack in the specimen makes the input bar-specimen interface (x_1 in Fig.1) essentially equivalent to a free boundary. When the incident wave reaches this interface, it will be completely reflected back into the input bar ($\sigma_t(x_1,t)= -\sigma_i(x_1,t)$ and $\sigma_t(x_1,t)=0$) until the specimen is stretched. The duration (ΔT) of internal reflection of the incident wave is related to the slack ΔL and the particle velocity at interface x_1. During ΔT, the force at interface x_1 is zero ($\sigma(x_1,t) = \sigma_i(x_1,t) + \sigma_r(x_1,t) = 0$), and the velocity at x_1 can be derived from the strain generated by the incident wave in the input bar and the elastic wave speed ($v(x_1,t) = 2C_0\varepsilon_i(t)$). Thus, ΔL is easily determined from the product of ΔT and $v(x_1,t)$. Consider the simple case when the striker has the same cross-sectional area and material as the input bar; $v(x_1,t)$ is then equal to the impact velocity of the striker (V_0) until the slack in the specimen is removed. For example, a ΔT of about 100 μs and a V_0 of around 12m/s would correspond to a ΔL of approximately 1.2mm. It should be noted that an exact knowledge of ΔL is not a critical, because its value is not involved in the calculation of stress or strain. This initial-slack approach can be carried out by gently stretching a ligament specimen between the input and output bars, then moving the bars back a little closer together. The resulting ΔL should not be excessive; otherwise, the incident wave may not be sufficiently long to accommodate the removal of the initial slack as well as stretching the specimen to failure. In this approach, the portions of the incident and reflected waves associated with loading on the specimen are different from that in traditional Hopkinson bar testing, whereby the entire durations of the signals recorded by the strain gages are used. As the values of ΔL and V_0 cannot be determined exactly, they cannot be used to calculate ΔT. If the specimen is stiff, ΔT can be ascertained directly from the reflected wave by identifying the onset of loading on the specimen (corresponding to a departure of the reflected wave from a constant amplitude associated with removal of the initial slack), as exemplified by *C-D* in Fig.3. The portion of the incident wave corresponding to loading of the specimen then starts at point *B*, ΔT from *A*. The front of the incident and reflected wave associated with actual loading of the specimen can be considered to have a vertical rising slope, commencing at points *B* and *D* respectively. Possible wave dispersion in the initial portion of the loading wave and the effects of a gradual rising edge are decreased or eliminated. However, note that point *D* in Fig.3 is quite difficult to identify in this case, as the specimen was extremely soft.

It is evident from Fig. 3, that the amplitude of the reflected wave $\varepsilon_r(t)$ is almost constant and equal to that of the incident wave $\varepsilon_i(t)$ because the transmitted wave is extremely small. This makes calculation of the average stress $\sigma_s(t)$ using Eq. (1) untenable, because the error resulting from the addition $\varepsilon_i(t)+\varepsilon_r(t)$ is too large. This is a common problem in the testing of compliant materials, and usually only the incident and transmitted waves are used to derive the stress and strain (assuming uniformity of stress within the specimen). In this study, the ligament specimens are short and relatively long input/output bars are employed; consequently the method of calculating the stress, strain and strain rate is simplified to using only two waves, i.e. omitting the reflected wave.

$$\sigma_s(t) = \frac{A_0}{A_s}\left[\sigma(x_2,t)\right] = \frac{E_0 A_0}{A_s}\left[\varepsilon_t(t)\right]$$
$$\dot{\varepsilon_s}(t) = \frac{v(x_1,t) - v(x_2,t)}{L_s} = \frac{2C_0}{L_s}\left[\varepsilon_i(t) - \varepsilon_t(t)\right] \qquad (2)$$
$$\varepsilon_s(t) = \int_0^t \dot{\varepsilon_s}(t)dt = \frac{2C_0}{L_s}\int_0^t \left[\varepsilon_i(t) - \varepsilon_t(t)\right]dt$$

The stress history is derived solely from the transmitted wave and the strain history is determined primarily from the incident wave; this is precisely why accuracy of the recorded transmitted wave is crucial in the testing of ligaments. Determination of the portion of the experimental signal to be used in Eq. (2) is now described. As illustrated in Fig.3, the time interval between the commencements of the entire incident wave (point *A*) and the transmitted wave (point *E*) can be divided into three segments. ΔT_1 denotes the time taken by the incident wave to travel from the strain gage on the input bar to the input bar-specimen interface x_1; ΔT_2 denotes the time taken by the transmitted wave to travel from the specimen-output bar interface x_2 to the strain gage on the output bar. Consequently, ΔT_3 is the sum of the specimen slack reduction time ΔT and the time taken for the load to travel through the specimen. $\Delta T_1$and ΔT_2 can be calculated accurately from the positions of the strain gages and the specimen, and the elastic wave speed of the bars. Thus, in Eq. (2), the starting points of the incident and transmitted waves can be associated with *A* and *F* respectively. As ΔT has been included in ΔT_3, the stress-strain curve derived from the signals starting at *A* and *F* will have an initial zero-stress phase that must be discarded. The other key consideration in this initial slack approach is how to ensure that the ultimate point in the stress-strain curve corresponds to failure of the specimen, rather than premature unloading because of the shortened loading duration/wave on the specimen. This can be ascertained by point *G* in Fig.3, the end of the transmitted wave corresponding to unloading that follows the end of the incident wave. Point *G* is located a distance of ΔT_i after point *F* (i.e. the duration of the entire incident wave). If the peak of the transmitted wave occurs before point *G*, this indicates that the specimen fails before the end of the loading wave arrives at the input bar-specimen interface and the stress-strain curve derived is valid.

(3) Generation of a sufficiently long loading pulse

In this study, the gage length of a bone-ligament-bone type specimen is defined as the distance between the centers of the ligament-bone connections. The gage length varies with the type and anatomic location of the ligament, and this results in a wide range of values, from 3mm to 22mm. Therefore, a sufficiently long loading wave is necessary to stretch these compliant specimens to failure, to obtain a complete stress-strain curve. In a traditional Hopkinson bar device, the cross-sectional area and material of the striker are similar to that of the input bar; thus, the length of the incident wave corresponds to twice the length of the striker. Therefore, a direct method of increasing the loading duration is to use a longer striker. However, this is limited by space constraints. The longest striker used in this study is one meter in length and this corresponds to an incident wave of 400μs duration. If ΔT is assigned a value of 100μs using the initial-slack approach and the striker velocity V_0 is 12m/s, the actual loading wave can induce about 3.6mm of specimen deformation. This corresponds to about 72% strain for a specimen with a gage length of approximately 5mm, which usually exceeds the failure strain. Thus, ligaments with small gage lengths (ALL, PLL) were tested using this method and the results showed that all specimens attained failure. Fig. 3 illustrates a test on an anterior longitudinal ligament specimen; the transmitted wave shows that the ligament reached its ultimate stress within the actual loading duration.

For other types of ligaments with longer gage lengths or high extensibility, a 400μs duration incident wave cannot ensure that specimens are loaded to failure. In employing the initially-slack specimen approach, a longer incident wave allows larger values of ΔL or ΔT to ensure a zero pre-load on the specimen. Consequently, a method was formulated to generate a longer incident wave, with a duration of around 1000μs. In a traditional Hopkinson bar set-up, the mechanical impedances of the striker and the input bar are often made equal through similarity in cross-sectional area and material. This results in the striker coming to rest after the stress wave generated upon impact travels to the other end of the striker and back. In contrast, the method proposed in this study employs a thick, heavy tubular striker to impact a light, thin input bar. Consider the impact of the striker on the input bar and the resulting elastic wave propagation, as illustrated in Fig. 4a. The integer *n* denotes the instants on the time axis that there is a change in the stress and velocity at the striker-bar interface (*n* = 1, 2, 3 …) – i.e. the instant of impact (*n* = 1) and the subsequent returns of the wave generated to the interface. After the first return of the stress wave in the striker to the impact interface (*n* = 2), the striker will continue to load the input bar at a reduced velocity of V_3, (i.e. V_{2n-1}), while the common particle velocity at the interface reduces from V_2 to V_4 (i.e. $V_{2(n-1)}$ to V_{2n}). This sustained loading (corresponding to subsequent striker velocities of V_3, V_5, …) will persist until the interfacial stress reduces to zero. Loading of the input bar would thus comprise several steps of decreasing amplitude, defined by σ_{2n} ; i.e. σ_2, σ_4 …, with the duration of each step being twice the time taken for the wave to traverse the striker length. If the wave impedance of the striker ($Z_s = \rho_s C_s A_s$) is much larger than that of the input bar (Z_i), then the steps will be very small and the decrease in stress gradual. The amplitude of the stress in each step of the incident stress is denoted by σ_{2n} and this is generated by the striker with a velocity of V_{2n-1} before the n^{th} loading cycle. The values of V_{2n-1} and σ_{2n} can be determined from:

$$V_{2n-1} = V_1 \cdot \left(1 - \frac{2Z_i}{Z_i + Z_s}\right)^{n-1} \quad (3)$$

$$\sigma_{2n} = V_1 \cdot \left(1 - \frac{2Z_i}{Z_i + Z_s}\right)^{n-1} \cdot \frac{Z_i Z_s}{Z_i + Z_s} \quad (4)$$

where V_1 is the initial striker impact velocity. In the present investigation, a one-meter long, thick steel tubular striker (30mm outer diameter, 12.8mm inner diameter) was used to impact a cap attached to the end of a 12.5mm diameter solid aluminum input bar. The wave impedance of the striker is around fourteen times that of the input bar. From Eq. (4), the amplitude of the incident wave induced decreases by a factor of about 13% between each step; this concurs with the signals shown in Fig.4b. If the cross-sectional area of the striker is much larger than the input bar, then the steps would be smaller, making the loading wave more constant. However, the configuration described corresponds to the limits of the existing equipment; this produces a step duration of around 400μs and a 1000μs long effective incident wave (equivalent to using a 2.5m long striker in a traditional set up) before superposition of the reflected wave from the input bar-specimen interface occurs. The length of the effective incident wave is twice the distance between the interface x_1 and the strain gage on the input bar (2.5m in the current setup). The consequence of this particular approach is that the entire reflected wave is superposed by the rear portion of the incident wave. This does not introduce problems in tests on ligaments, because only the incident and transmitted waves are used in calculating the results (Eq.2). The stress history of the specimen is derived solely from the transmitted wave, and the strain rate is obtained from the (usable) initial portion of the incident wave. Variation in the strain rate associated with the small steps in the incident wave is too small to be significant. As the stepped incident wave has a steep rising edge and a constant amplitude during the initial (and subsequent) step, it is just as effective as an incident wave generated by the traditional approach if the specimen is short and breaks within the first step. Moreover, the modified method yields a long loading duration that can accommodate failure of very compliant specimens.

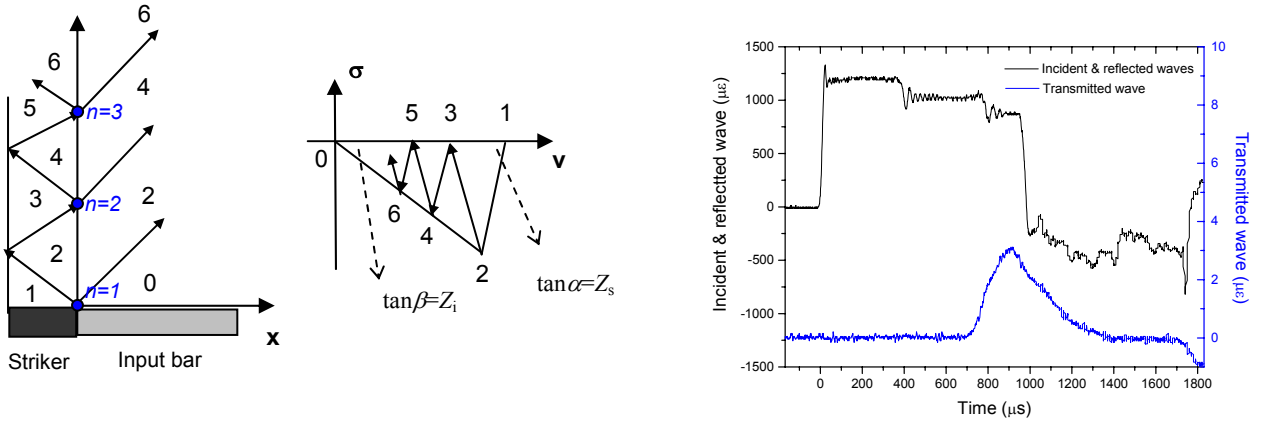

(a) Illustration of wave propagation in impact of a thick steel bar on a thin aluminium input bar.

(b) Input/output bar strain signals in a test on an interspinous ligament

Fig. 4 Method for generation of long incident wave

Determination of dynamic properties

Ligaments were extracted from three male cadavers, denoted by P1 (aged 40), P2 (aged 65) and P3 (aged 69). The number of specimens that can be harvested from a cervical spine is quite limited; for example, there are only two pieces of *alar* ligaments and one piece of transverse ligament. The tensile strain rate imposed on each type of ligament was of the order of 10^2~10^3/s, corresponding to a stretch velocity of 10~12m/s. The test results show characteristic stress-strain profiles and significant strain-rate sensitivity. Fig. 5 illustrates the mechanical responses of four *alar* ligaments harvested from two cadavers (P1 and P3). From each cadaver, one of the two specimens was subjected to dynamic tension and the other to static loading; both were taken to failure. The curves exhibit the characteristic nonlinear initial toe region, followed by an almost linear elastic region, then final rupture. The pre-failure profiles are similar, but the post-failure trends vary. Quasi-static responses show a long toe region with a lower stiffness, while dynamic loading of the ligament from the same cervical spine yields stiffer behavior, a higher strength, but smaller elongation. After attaining the ultimate stress, the stress drops rapidly, indicating sudden failure of the ligament sample. For the static responses, the one from cadaver P1 (aged 40) shows a higher stiffness; while in the dynamic tests, the one from cadaver P3 (aged 69) attained a higher ultimate stress, although the stress-strain curve shows that damage commences at a value approximately half of this (indicated by the kink in the stress-strain curve). This indicates that age is not the only governing factor, but that there may also be differences in the characteristics of ligaments from a given source, which are inherent to the particular individual. Despite the inherent scatter in the results

obtained, the strain rate sensitivity of ligaments is obvious from the stress-strain profiles. This is clearly evident in Fig. 6, which shows results of tests on transverse ligaments. In these tests, the single transverse ligament extracted from each cadaver (P1, P2 and P3) was first subjected to static tension, within the linear elastic response, using an Instron Micro tester. This was repeated a second time. The specimen was then mounted on the Hopkinson bar and subjected to dynamic stretching till rupture. The stress-strain curves from the two static tests are close to each other, confirming that no damage was induced. As the bone-ligament-bone specimen configuration was maintained in both static and dynamic tests, the large difference in response in the toe region and the subsequent stress levels, arising from static and dynamic loading, can be attributed to rate sensitivity of ligament material. The stiffness increases significantly under dynamic loading. The effect of age is not apparent from tests on the four *alar* ligaments; however, this is not true for transverse ligaments. The TL from cadaver P1 (aged 40) has a larger dynamic ultimate stress/strain (19.04MPa / 8.44%) than the other two from older cadavers (P2: 12.81MPa / 5.47%; P3: 13.58MPa / 6.20%); the static stiffness decreases with age, but the dynamic stiffnesses are quite similar.

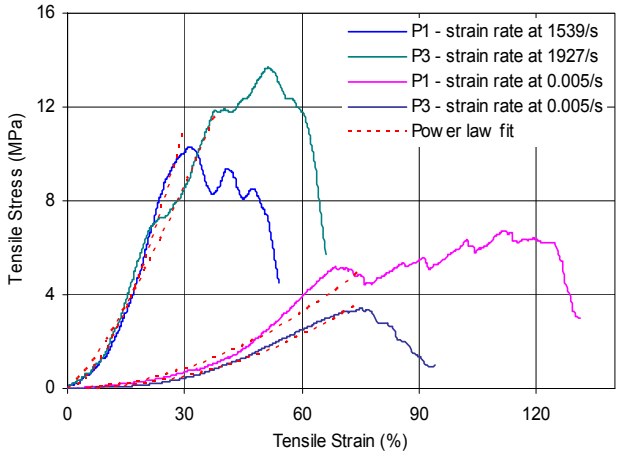

Fig.5 Static and dynamic tensile stress-strain behavior of *alar* ligament specimens, together with power law fits till failure.

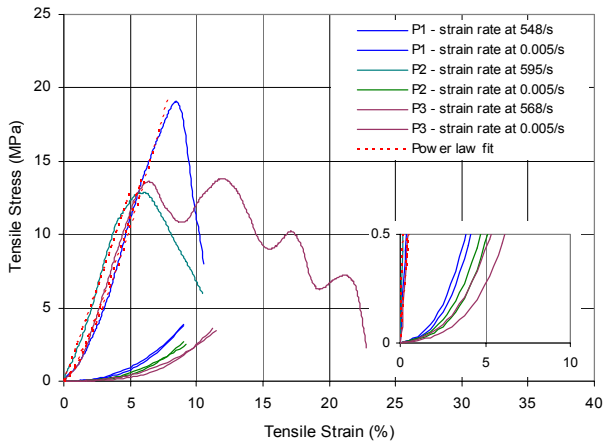

Fig.6 Static and dynamic tensile stress-strain behavior of transverse ligament specimens, together with power law fits till failure (initial response magnified in window).

In modeling the nonlinear response of soft bio-tissues, curve-fitting via empirical equations is adopted for simplicity and ease of subsequent use. The regression quality was generally found to be quite good. Elliott and Setton [24] used a bilinear equation to relate stress (σ) and strain ($\varepsilon_{\alpha\alpha}$) for the toe region and the subsequent linear response of the annulus fibrosus in the lumbar disc. Yoganandan et al. [14] listed the two moduli and transition strain for ligaments from the human cervical spine. Such bilinear fits were also used to approximate the stress-strain response of collagen fibril in ligaments, e.g. Kwan and Woo [25]. Apart from linear approximations, higher order polynomials have also been employed; Savelberg et al [26] used a second degree polynomial ($F = aL^2 + bL + c$) to fit the load (F) versus deformation (L) response for human wrist ligaments; Carlstedt and Skagervall [27] defined the load-deformation behavior of plantaris longus tendons in rabbits using a modified polynomial equation ($P = a\varepsilon + b\varepsilon^3$) to minimize the number of parameters. In this study, the following power law was employed:

$$\sigma = a \cdot \varepsilon^{b} \qquad (5)$$

This power law relationship was found to be capable of describing both the static and dynamic responses of most of the ligaments from the human cervical spine. This power law fit has also been used previously in describing nonlinear properties of soft bio-tissues such as tendons [28, 29] and vertebral discs [30]. The quality of fit corresponding to these empirical equations was found to be quite good for ligaments prior to failure, as illustrated in Fig.5 and Fig.6.

Conclusion

An experimental protocol based on use of a split tensile Hopkinson bar device has been established for high strain rate testing of compliant biological material specimens. This enables information on the dynamic mechanical behavior of cervical spine ligaments to be obtained and contributes to addressing the scarcity of information in this area. The proposed modifications to traditional Hopkinson bar test techniques proved useful for accommodating soft bio-tissue samples with high extensibility and extremely low wave impedance characteristics. Modifications incorporated include a means to capture transmitted waves of small amplitude, an initial-slack approach to ensure no preloading of specimens so that the complete response in the initial toe regime can be obtained, and generation of a sufficiently long incident wave to stretch high-elongation specimens to failure, without exceeding practical space constraints. This facilitated the study and testing of human cervical spine ligaments to obtain their stress-strain characteristics at strain rates corresponding to 10^2/s~10^3/s. Significant rate sensitivity was observed in

dynamic loading, which also shortens the initial toe regime, elevates stress levels and reduces the amount of extension before failure. The proposed experimental method is envisioned to be useful in studies related to ligament injuries arising from suddenly-applied loads.

References

[1] Noyes, F.R., Delucas, J.L., Torvik, P.J. Biomechanics of anterior cruciate ligament failure: an analysis of strain-rate sensitivity and mechanisms of failure in primates. The Journal of Bone and Joint Surgery. Vol. 56-A, No.2, pp.236-253, 1974.

[2] Peterson, R.H., Woo, S.L-Y. A new methodology to determine the mechanical properties of ligaments at high strain rates. Journal of Biomechanical Engineering. Vol. 108, pp.365-367, 1986.

[3] Haut, T.L., Haut, R.C. The state of tissue hydration determines the strain-rate-sensitive stiffness of human patellar tendon. J. Biomechanics, Vol.30, No.1, pp.79-81, 1997.

[4] Wren, T.AlL., Yerby, S.A., Beaupré, G.S., Carter, D.R. Influence of bone mineral density, age, and strain rate on the failure mode of human Achilles tendons. Clinical Biomechanics 16, pp.529-534, 2001.

[5] Crowninshield, E.D. and Pope, M.H. The strength and failure characteristics of rat medial collateral ligaments. The Journal of Trauma. Vol.16, No.2, pp.99-105, 1976.

[6] Moroney, S.P., Schultz, A.B., Miller, J.A.A. and Andersson, G.B.J. Load-displacement properties of lower cervical spine motion segments, J. Biomechanics, Vol.21, No.9, pp.769-779, 1988.

[7] Crisco III, J.J., Panjabi, M.M., and Dvorak, J. A model of the alar ligaments of the upper cervical spine in axial rotation. J. Biomechanics, Vol.24, No.7, pp.607-614, 1991.

[8] Nightingale, R.W., Winkelstein, B.A., Knaub, K.E., et.al. Comparative strengths and structural properties of the upper and lower cervical spine in flexion and extension. Journal of Biomechanics 35, pp. 725-732, 2002.

[9] Yoganandan, N., Pintar, F., Cusick, J.F. Biomechanical analyses of whiplash injuries using an experimental model. Accident Analysis and Prevention, Vol. 34, pp.663-671, 2002.

[10] Yoganandan, N., Pintar, F.A. Inertial loading of the human cervical spine. Journal of Biomechanical Engineering, Vol.119, pp.237-240, 1997.

[11] Panjabi, M.M., Cholewicki, J., Nibu, K., Babat, L.B., Dvorak, J. Spine. Vol.23, No.1, pp.17-24, 1998.

[12] Chazal, J., Tanguy, A., Bourges, M., Gaurel, G., Escande, G., Guillot, M., Vanneuville, G. Biomechanical properties of spinal ligaments and a histological study of the supraspinal ligament in traction. J. Biomechanics. Vol.18, No.3, pp.167-176, 1985.

[13] Myklebust, J.B., Pintar, F., Yoganandan, N., et. al. Tensile strength of spinal ligaments. Spine, Vol.13, No.5, pp.526-531, 1986.

[14] Yoganandan, N., Kumaresan, S., Pintar, F.A. Geometric and mechanical properties of human cervical spine ligaments. Journal of Biomechanical Engineering, Vol.122, pp.623-629, 2000.

[15] Yoganandan, N., Pintar, F., Butler, J. et.al. Spine, Vol. 14, No.10, pp.1102-1109, 1989.

[16] Panjabi, M.M., Crisco III, J.J., Lydon, C., Dvorak, J. The mechanical properties of human alar and transverse ligaments at slow and fast extension rates. Clinical Biomechanics, Vol. 13, NO.2, pp.112-120, 1998.

[17] Clark, C.R., et al. Chapter1: Anatomy of the cervical spine. The cervical spine, 3rd edition, ISBN 0397515359, 1998.

[18] Riemersma, D.J., Schamhardt, H.C. The Cryo-jaw, a clamp designed for in vitro rheology studies of horse digital flexor tendons. Journal of Biomechanics 15, 619-620, 1982.

[19] Lindholm, U.S., in R.F. Bunshah (Ed.), Techniques in metals research, Vol. 5. Part 1, Interscience, New York, 1971.

[20] Kolsky, H. An Investigation of the mechanical properties of materials at very high rates of loading. Proceedings of the Physical Society, B62, 676-701, 1949.

[21] Chen, W., Zhang, B., Forrestal, M.J. A split Hopkinson bar technique for low-impedance materials. Experimental Mechanics, Vol. 39, No. 2, 81-85, 1999.

[22] Wang L.L., Labibes, K., Azari, Z., Pluvinage, G. Generalization of split Hopkinson bar technique to use viscoelastic bars. Int. J. Impact Engng, Vol. 15, No. 5, 669-686, 1994.

[23] Zhao, H., Gary, G., Klepaczko, J.R. On the use of a Viscoelastic split Hopkinson pressure bar. Int. J. Impact Engng, Vol. 19. No. 4. 319-330, 1997.

[24] Elliott, D.M., Setton, L.A. Anisotropic and inhomogeneous tensile behavior of the human annulus fibrousus: experimental measurement and material model predictions. Journal of Biomechanical Engineering, 123, 256-263, 2001.

[25] Kwan, M.K., and Woo, S.L-Y. A structural model to describe the nonlinear stress-strain behaviour for parallel-fibered collagenous tissues. Journal of biomechanical engineering, Vol. 111, pp.361-363, 1989.

[26] Savelberg, H.H.C.M., Kooloos, J.G.M., Huiskes, R., Kauer, J.M.G. An indirect method to assess wrist ligament forces with particular regard to the effect of preconditioning. Journal of Biomechanics, 26, 1347-1351, 1993.

[27] Carlstedt, C.A. and Skagervall, R. A model for computer-aided analysis of biomechanical properties of the plantaris longus tendon in the rabbit. Journal of Biomechanics Vol.19, PP.251-256, 1986.

[28] Morgan, F.R. The mechanical properties of fibers: Stress-strain curves. J. Soc. Leath. Trades , 170-182, 1960.

[29] Elden, H.R. Physical properties of collagen fibers. International review of connective tissue research (Edited by Hall, D.A.), Vol. 24, pp. 283-348. Academic Press, New York, 1968.

[30] Klisch, S.M. and Lotz, J.C. A special theory of ibphasic mixtures and experimental results for human annulus fibrosus tested in confined compression, Journal of Biomechanical Engineering, 122, 180-188, 2000.